Analysis and Classification of Vibroarthographic Signal Using Nonstationary Signal Processing Techniques

Saif Nalband
2013PHXF0008G

Supervisor
Dr. A. Amalin Prince

Co-Supervisor
Dr. Anita Agarwal

January 18, 2018

Overview

Motivation

- The knee joint is one of the most complex, the strongest and most important joints in the human body[1].
- India may become the osteoarthritis hub with more than 65 million cases by 2025 according to studies conducted by medical professionals [2].
- the limitations and drawbacks of imaging techniques and arthroscopy have prompted researchers for alternative solutions such as Vibroarthrographic(VAG) [3, 4].

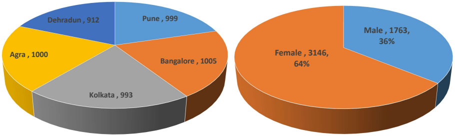

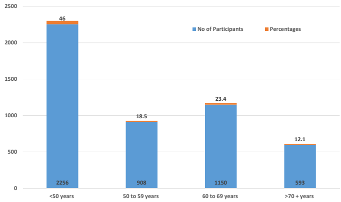

Figure 1: Statistical study [2]

The characteristics of VAG signal

i. VAG signal is a multicomponent signal.
ii. VAG signal is nonstationary in nature.
iii. VAG signal is aperiodic and non-linear.

Sensors used for acquiring VAG signals

- Microphone [5]
- Accelerometer [6].

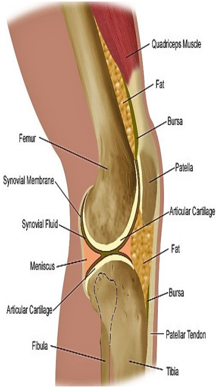

Figure 2: Anatomy of Knee joint

A Computer aided diagnostic(CAD) system

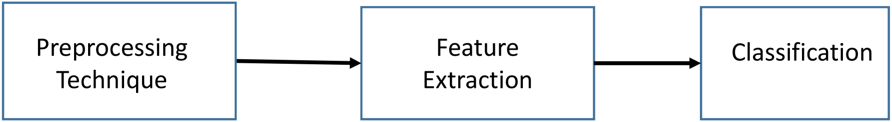

Figure 3: A Computer aided diagnostic(CAD) system [7]

Literature Review: Preprocessing

Table 1: Preprocessing Techniques

Linear Signal Processing

Year	Author	Techniques	Features	Classifier	Accuracy%
1994	Zhang[8]	**two-stage least-mean-squares (LMS)**	-	-	-
1997	Krishnan[9]	**adaptive segmentation using RLSL**	AR coefficients, VMS	Logistic classification	68.9
2013	Wu[10]	**adaptive time-delay neural filter**	-	-	-

Nonlinear Signal Processing

year	Author	Techniques	Features	Classifier	Accuracy%
2012	*Chen[11]	**ICA**	root mean square	-	-
2015	Sundar[12]	**VMD**	-	-	-
2013	Wu[13]	**EMD**	turn counts	-	-
2013	Wu[14]	**EEMD**	-	-	-
2016	Wu[15]	**EEMD**	Entropy, EAM	LS-SVM	83.56

*Different dataset

Literature Review: Feature Extraction

Table 2: Feature Extraction

Year	Author	Techniques	Features	Classifier	Accuracy%
1995	Tavitha[16]	Fixed segmentation & linear prediction modelling	**model parameters, dominant poles, spectral power ratio**	-	-
1996	Moussavi[17]	recursive least squares	**six AR coefficients, VMS, age etc.**	leave-one-out	71.1
1997	Rangayyan[18]	adaptive segmentation using RLSL	**6 Dominant poles & cepstral coefficients**	LRA	75.6
1997	Krishnan[9]	adaptive segmentation using RLSL	**AR coefficients,VMS**	leave-one-out	68.9
2007	Wu[19]	PDF + histogram	**FF,mean, turn counts**	NN	0.82 AUC
2010	Wu [20]	Parzen Window	**FF,mean, turn counts**	NN	77.53
2013	Wu[21]	Bivariate Probability Distribution Modeling	**FF,mean, turn counts**	maximal posterior probability	86.6
2013	Wu[22]	Wavelet MP segmented	**no MP atoms & significant turns**	dynamic weighted fusion (DWF)	88
2013	Wu[23]	power spectral analysis	**Fractal dimension**	RBF NN	0.74 AUC
2014	Wu[24]	bivariate Gaussian kernels	**fractal scaling index,EAM**	Bayesian decision	0.95 AUC

Literature Review: Time Frequency Analysis

Table 3: Time Frequency Techniques

Year	Author	Techniques	Features	Classifier	Accuracy%
1997	Krishnan[25]	**wavelet matching pursuit**	energy, frequency	discriminant analysis	77.8
2000	Krishnan[26]	**adaptive matching pursuit decomposition**	energy, frequency	LRA	68.90
2006	Umapthy[27]	**modified local discriminant**	normalized node energy, correlation coffecients	LDA	79.8
2009	Wu[28]	**wavelet MP segmented**	no of MP atoms and significant turns	LS-SVM	73.03
2009	*Kim[29]	**dynamic time warping**	energy and frequency	NN	91.4
2013	*Chen[30]	**HHT**	-	NN	85.3
2015	*Backowiz[31]	**STFT**	-	-	-

*Different dataset

Literature Review: Feature Selection & Classifier

Table 4: Feature Selection & Classifier

Feature Selection

Year	**Author**	**Techniques**	**Features**	**Classifier**	**Accuracy%**
2008	Wu [32]	PDF + histogram	FF,mean, turn counts,VMS	NN	0.91 AUC
2013	Wu[23]	power spectral analysis	FF,mean, turn counts, VMS,fractal dimension	RBF NN	0.92 AUC

Classifier

Year	**Author**	**Techniques**	**Features**	**Classifier**	**Accuracy%**
2007	Mu[33]	PDF + histogram	FF,mean, turn counts	**Strict 2 surface classifier**	0.95 AUC
2011	Wu[34]	Parzen Window	FF,mean, turn counts	**LS-SVM**	80.90
2014	Wu[35]	PDF + histogram	FF,mean, turn counts	**k-nearest neighbour (k-NN)**	80

Gaps identified

Following research gaps have been identified:

- ✓ Preprocessing of VAG signals using nonstationary linear preprocessing technique : Wavelet Packet Decomposition [36].
- ✓ Preprocessing of VAG signals using nonstationary nonlinear preprocessing technique : complete ensemble empirical mode decomposition with adaptive white noise (CEEMDAN) [37].
- ✓ Entropy based features, recurrence quantification analysis [38], feature based on central tendency measure (CTM) [39] and statistical parameters.
- ✓ Feature selection techniques : Genetic algorithm [40] and apriori algorithm [41].
- ✓ Time frequency analysis using smoothed pseudo WignerVille distribution (SPWVD)[42] and Hilbert-Huang transform (HHT)[43].

Objective Of Thesis

1: *To analyse VAG signals using nonstationary linear signal processing technique and to extract entropy and recurrence quantification analysis(RQA) based features.*

2: *To identify the most significant and relevant features by feature selection algorithms for building effective classification model.*

3: *To analyse VAG signals using nonstationary nonlinear signal processing techniques and to extract entropy based features and feature based on central tendency measures (CTM).*

4: *To analyse VAG signals by time-frequency distribution using smoothed pseudo WignerVille distribution (SPWVD) and Hilbert-Huang transform (HHT) and to extract statistical features.*

Thesis structure

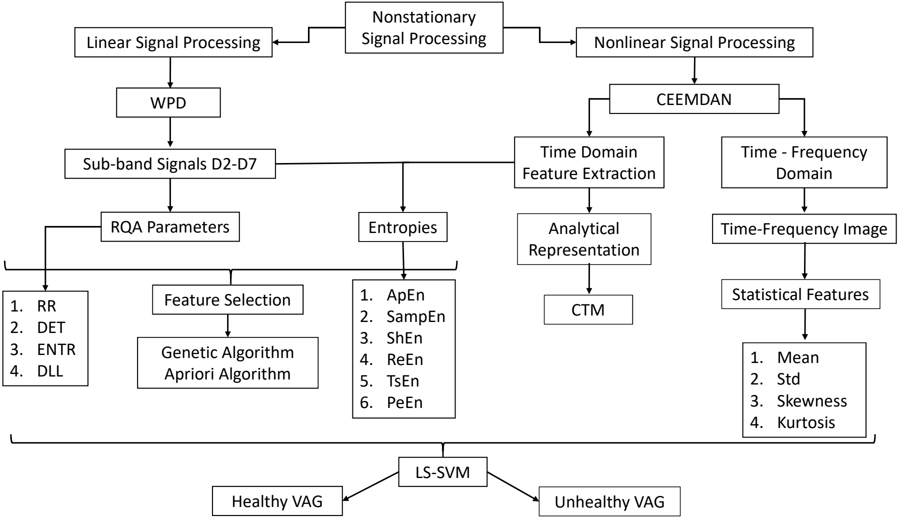

Figure 4: Thesis structure

Data set used in the thesis

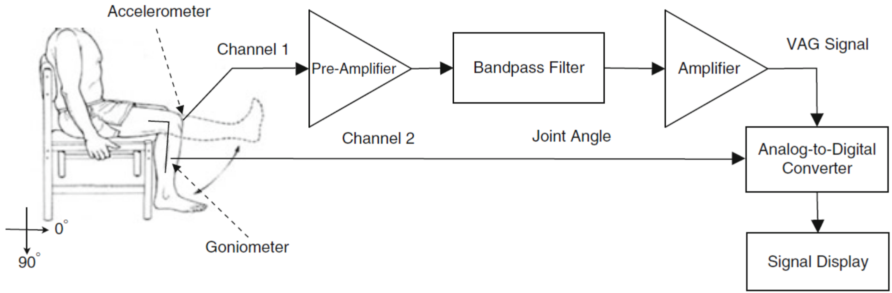

Figure 5: VAG data acquisition system. Image taken from Wu Y. Knee joint vibroarthrographic signal processing and analysis. Springer; 2015 Jan 29 [4].

- Rangayyan *et al.* carried out the data acquisition of VAG signals using a miniature accelerometer[18].
- In our study, the analysis of VAG signal has been carried out using the data set acquired by Rangayyan *et al.*

A sample of raw VAG signal

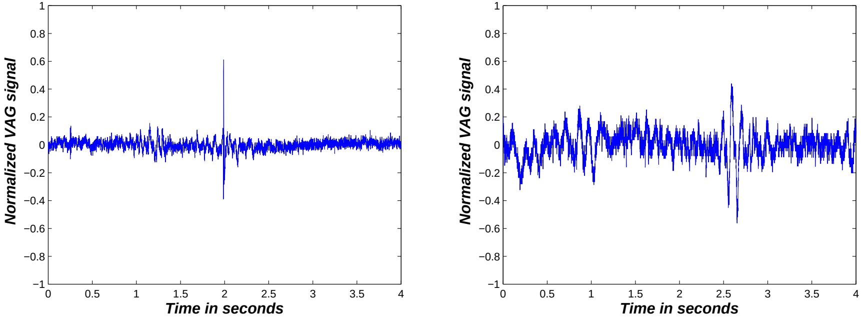

(a) Healthy subject

(b) Unhealthy subject

Figure 6: Sample raw VAG signal

A sample of filtered VAG signal

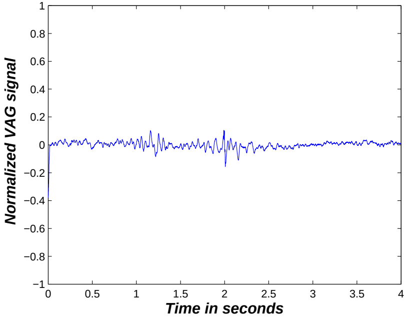

(a) Healthy subject

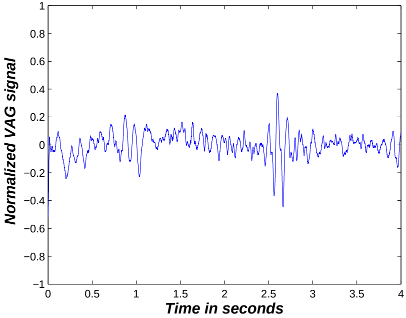

(b) Unhealthy subject

Figure 7: Filtered VAG signal using double cascaded moving average filter

The proposed methodology

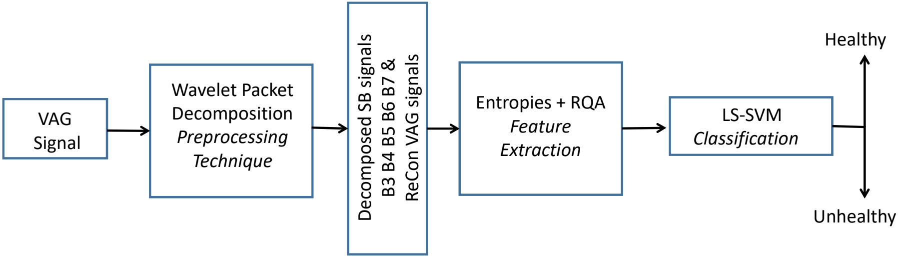

Figure 8: Block diagram for diagnosis of knee joint disorders using VAG signals

Saif Nalband, Aditya Sundar, A. Amalin Prince, Anita Agarwal: "Feature selection and classification methodology for the detection of knee-joint disorders". Computer Methods and Programs in Biomedicine 127: 94-104 (2016)

Wavelet Decomposition of VAG signal

Table 5: Decomposition of the VAG signal into subband signals

Decomposed Signal	Frequency	Decomposed Signal	Frequency
B1	500-1000 Hz	B6	15.62-31.25 Hz
B2	250-500 Hz	B7	7.81-15.62 Hz
B3	125-250 Hz	B8	3.90-7.81 Hz
B4	62.5-125 Hz	B9	1.95-3.90 Hz
B5	31.25-62.5 Hz	B10	1-1.95 Hz
A10	0-1 Hz		

Feature Extraction

Ten features are extracted and they are

Entropy	Recurrence quantification analysis(RQA)
Approximate entropy (ApEn)	Recurrence rate (RR)
Sample entropy (SampEn)	Determinism (DET)
Shannon entropy (ShEn)	Entropy (ENTR)
Rényi entropy (ReEn)	Averaged diagonal line length (DLL)
Tsallis entropy (TsEn)	
Permutation entropy (PeEn)	

Pattern Classification

- Least square support vector machine (LS-SVM) with RBF as kernel function.
- The performance of the pattern classification has been carried out using
  1) Sensitivity (SEN):
  2) Specificity (SPF):
  3) Accuracy (ACC):
  4) Positive predictive value (PPV)
  5) Negative predictive value (NPV)
  6) Matthews correlation coefficient (MCC)
  7) False Discovery Detection (FDR)
  8) Area under the receiver operating characteristic (AUC-ROC)

Results: Wavelet Decomposition of VAG signal

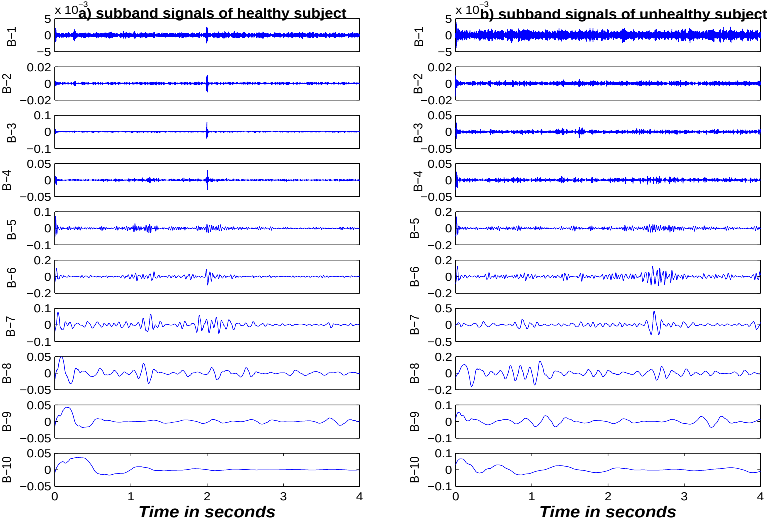

Figure 9: Wavelet decomposition of VAG signal for (a) healthy and (b)unhealthy subject

Results : Reconstructed VAG signal

The VAG signal is reconstructed from the subband signal (*B3, B4, B5, B6 and B7*) and is shown in figure 3.5.

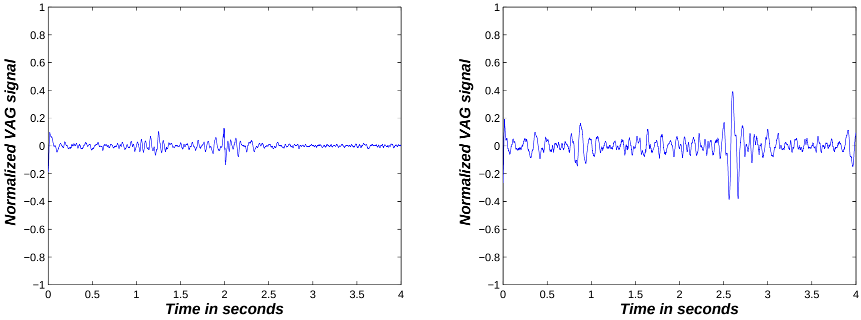

(a) Healthy subject (b) Unhealthy subject

Figure 10: Reconstructed VAG signals

Results: Statistical measures

Table 6: Statistical measures of ApEn extracted from subband signals

		Healthy Class	Unhealthy Class	
Features	Subband	Mean $\pm$ Std	Mean $\pm$ Std	p-value
ApEn	B3	0.6374 ± 0.0779	0.5768 ± 0.1772	0.0407
	B4	0.4766 ± 0.0753	0.4380 ± 0.1348	0.1192
	B5	0.3367 ± 0.0974	0.3127 ± 0.1336	0.2619
	B6	0.1668 ± 0.0631	0.2048 ± 0.1287	0.7951
	B7	0.0940 ± 0.0481	0.1221 ± 0.0806	0.1802

Results : Statistical measures

Table 7: Statistical measures of entropy and RQA based features extracted from reconstructed VAG signals

	Healthy Class	Unhealthy Class	
Features	Mean ± Std	Mean ± Std	p value
ApEn	1.7792 ± 0.1650	2.0113 ± 0.1303	2.421E-08
SampEn	2.3083 ± 0.1908	2.0744 ± 0.3727	1.7E-05
ShEn	5.0713 ± 0.4934	5.3087 ± 0.5355	0.0828
ReEn	4.4365 ± 0.5220	4.6323 ± 0.5849	0.1671
TsEn	0.9864 ± 0.0082	0.9886 ± 0.0066	0.1671
PeEn	1.7047 ± 0.1963	1.8260 ± 0.1467	0.0071
RR	0.2524 ± 0.0737	0.2885 ± 0.1391	0.3445
DET	0.9974 ± 0.0016	0.9967 ± 0.0026	0.2846
ENTR	3.3780 ± 0.5787	3.3725 ± 0.4149	0.6854
DLL	17.1224 ± 14.6281	14.7414 ± 6.3774	0.7632

Results: Statistical Boxplot

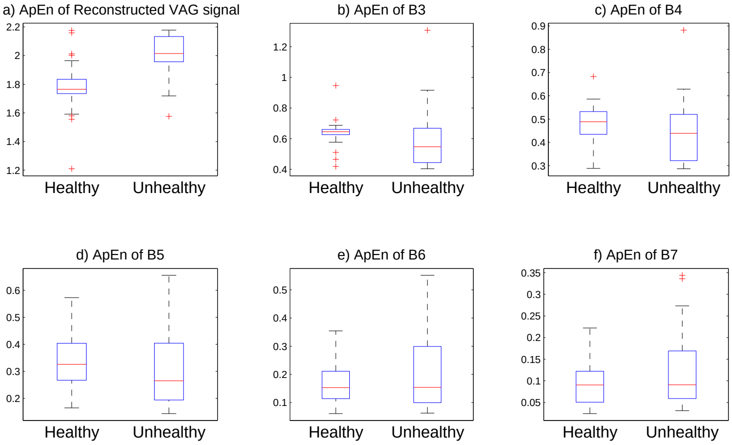

Figure 11: Boxplot of ApEn

Results: Classification

Table 8: Classification performance of extracted features from subband signals

Features	**ACC**	SEN	SPE	NPV	PPV	MCC	FDR	AUC-ROC
ApEn	**0.8315**	0.8205	0.8400	0.8101	0.8302	0.8571	0.2000	0.7663 ± 0.0524
SampEn	**0.8539**	0.8824	0.8158	0.8738	0.8484	0.8378	0.1346	0.7642 ± 0.0526
ShEn	**0.6292**	0.9216	0.2368	0.7402	0.4672	0.6923	0.3816	0.6780 ± 0.0574
ReEn	**0.6404**	0.9412	0.2368	0.7500	0.4721	0.7500	0.3766	0.7033 ± 0.0559
TsEn	**0.6854**	0.9216	0.3684	0.7705	0.5827	0.7778	0.3380	0.6899 ± 0.0577
PeEn	**0.8764**	0.9412	0.7895	0.8972	0.8620	0.9091	0.1429	0.7920 ± 0.0583
RR	**0.7865**	0.9423	0.5676	0.8376	0.7313	0.8750	0.2462	0.7848 ± 0.0565
DET	**0.7753**	0.8085	0.7381	0.7917	0.7725	0.7750	0.2245	0.9187 ± 0.0268
ENTR	**0.7978**	0.9804	0.5526	0.8475	0.7361	0.9545	0.2537	0.8668 ± 0.0391
DLL	**0.7079**	0.8431	0.5263	0.7679	0.6662	0.7143	0.2951	0.6367 ± 0.0627
All Features	**0.8090**	0.9216	0.6579	0.8468	0.7786	0.8621	0.2167	0.8606 ± 0.0397

Results: AUC-ROC for subband signals

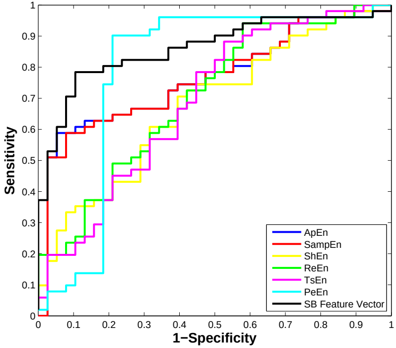

(a) ROC plot for entropy based features

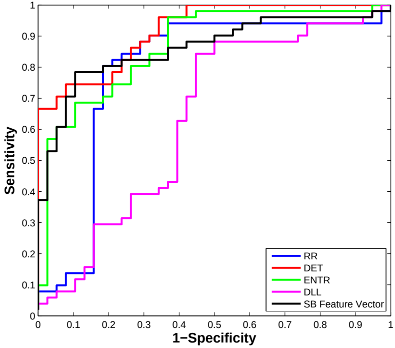

(b) ROC plot for RQA parameters

Figure 12: ROC plot for features extracted from subband signals

Results: Classification

Table 9: Classification performance of extracted features from reconstructed VAG signals

Features	ACC	SEN	SPE	NPV	PPV	MCC	FDR	AUC-ROC
ApEn	**0.7528**	0.7843	0.7105	0.7843	0.7465	0.7105	0.2157	**0.7791 $\pm$ 0.0514**
SampEn	**0.8202**	0.8235	0.8158	0.8400	0.8197	0.7750	0.1429	**0.8540 $\pm$ 0.0417**
ShEn	**0.6629**	0.7647	0.5263	0.7222	0.6344	0.6250	0.3158	**0.6501 $\pm$ 0.0583**
ReEn	**0.8315**	0.9804	0.6316	0.8696	0.7869	0.9600	0.2188	**0.6692 $\pm$ 0.0588**
TsEn	**0.7753**	0.8163	0.7250	0.8000	0.7693	0.7632	0.2157	**0.6011 $\pm$ 0.0601**
PeEn	**0.8132**	0.9508	0.5333	0.8722	0.7121	0.8421	0.1944	**0.8989 $\pm$ 0.0236**
RR	**0.7978**	0.7419	0.8276	0.7188	0.7836	0.8571	0.3030	**0.7069 $\pm$ 0.0551**
DET	**0.7528**	0.7353	0.7636	0.6944	0.7493	0.8235	0.3421	**0.6383 $\pm$ 0.0596**
ENTR	**0.6517**	0.7647	0.5000	0.7156	0.6183	0.6129	0.3276	**0.7312 $\pm$ 0.0528**
DLL	**0.7079**	0.8824	0.4737	0.7759	0.6465	0.7500	0.3077	**0.7461 $\pm$ 0.0548**
All Features	**0.8427**	0.9020	0.7632	0.8679	0.8297	0.8529	0.1636	**0.8560 $\pm$ 0.0427**

Results: AUC-ROC for reconstructed signals

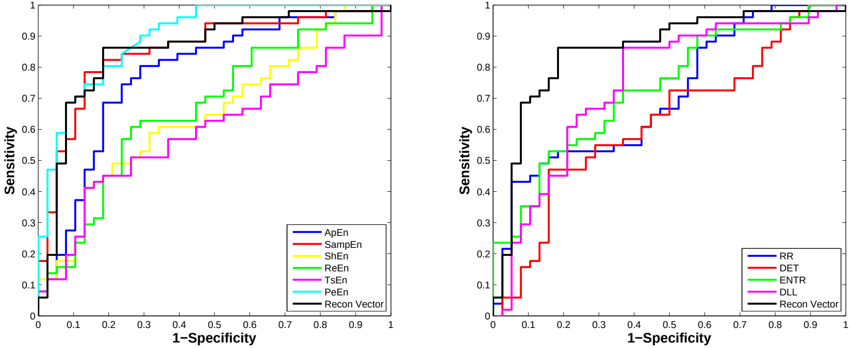

(a) ROC plot for Entropy based features (b) ROC plot for RQA parameters

Figure 13: ROC plot for features extracted from reconstructed signals

Conclusion

- Nonstationary linear signal possessing technique : WPD.
- Six entropy based features and four RQA parameters were extracted from subband and reconstructed VAG signals distinctly.
- **Fifty** features were extracted from the subband signals (*B3, B4, B5, B6, B7*) and **ten** from reconstructed VAG signal.
- The highest classification accuracy of **87.64%** was obtained for PeEn extracted from subband signals.

The proposed methodology

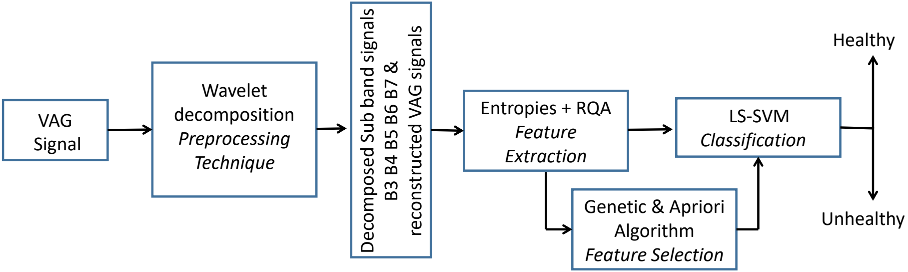

Figure 14: Block diagram for diagnosis of knee joint disorders using feature selection

Saif Nalband, Aditya Sundar, A. Amalin Prince, Anita Agarwal: "Feature selection and classification methodology for the detection of knee-joint disorders". Computer Methods and Programs in Biomedicine 127: 94-104 (2016)

Results: Genetic Algorithm

The optimal feature set constituted of eight features and they are:

1) ApEn of subband B7.
2) SampEn of subband B3.
3) SampEn of subband B7.
4) TsEn of subband B3.
5) TsEn of subband B7.
6) PeEn of subband B4.
7) ApEn of reconstructed signal.
8) SampEn of reconstructed signal.

Results: Apriori Algorithm

The feature set consisted of five features, which showed the maximum recurrence and they are

1) ApEn of subband B6.
2) ShEn of subband B6.
3) PeEn of subband B5.
4) ENTR (RQA) of subband B5.
5) SampEn of reconstructed signal.

Results: Classification

Table 10: Comparison of classification performance of FS algorithm

Attributes	All features vector	Features subband	Features ReCon	FS from GA	**FS from ApA**
No of features	60	50	10	8	**5**
ACC	**0.6966**	**0.8090**	**0.8427**	**0.8202**	**0.8539**
SEN	0.58882	0.9216	0.9020	0.7254	0.9272
SPE	0.8421	0.6579	0.7632	0.9473	0.7352
NPV	0.6038	0.8468	0.8679	0.72	0.862
PPV	0.8333	0.7786	0.8297	0.9487	0.85
MCC	0.4337	0.8621	0.8529	0.6707	0.6868
FDR	0.1667	0.2167	0.1636	0.0512	0.15
AUC-ROC	**0.7822 $\pm$ 0.0471**	**0.8606 $\pm$ 0.0397**	**0.8560 $\pm$ 0.0427**	**0.8754 $\pm$ 0.0347**	**0.9252 $\pm$ 0.0261**

Results: AUC-ROC

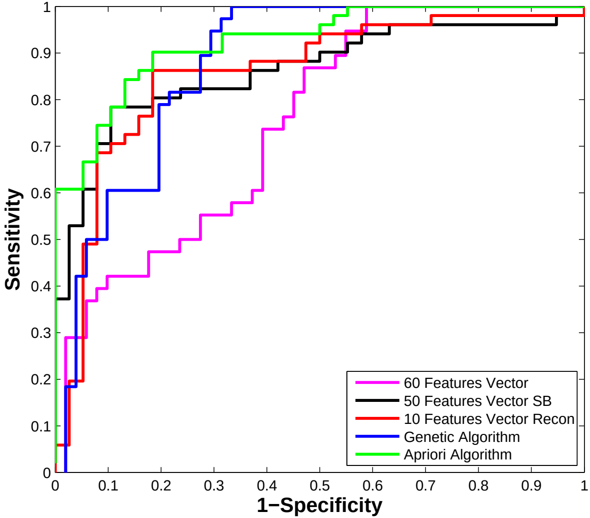

Figure 15: ROC plot of features selected from FS

Conclusion

- Feature selection algorithm has been used to discard the irrelevant and redundant features.
- Genetic algorithm selected eight features.
- Apriori algorithm selected five features
- Entropy based features were prominent features in comparison to RQA parameters.
- The highest classification of **85.39%** and AUC-ROC of **(0.9252 ± 0.0261)** was achieved by five features selected from the apriori algorithm.

The proposed methodology

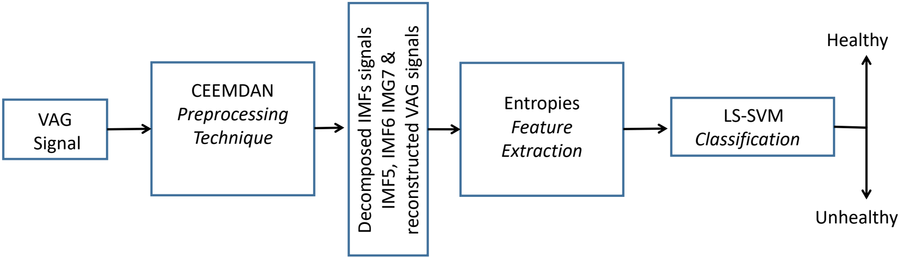

Figure 16: Block diagram for diagnosis of knee joint disorders using CEEMDAN

Saif Nalband, A. Amalin Prince, Anita Agarwal:"An entropy based feature extraction and classification of vibroarthographic signal using improved complete ensemble empirical mode decomposition with adaptive noise".(Manuscript Accepted: In Press) IET Science, Measurement & Technology 2017, DOI: 10.1049/iet-smt.2017.0284

Results: IMFs obtained by CEEMDAN

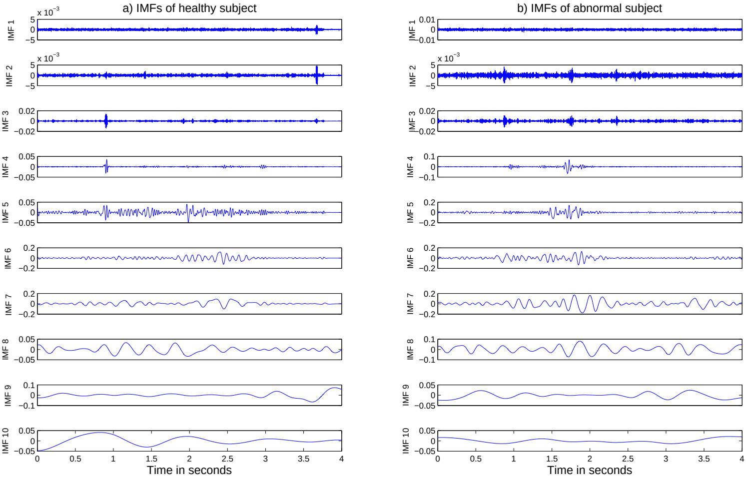

Figure 17: IMFs obtained from VAG signal of (a) healthy subject and (b) unhealthy subject

Results: Reconstructed VAG signal

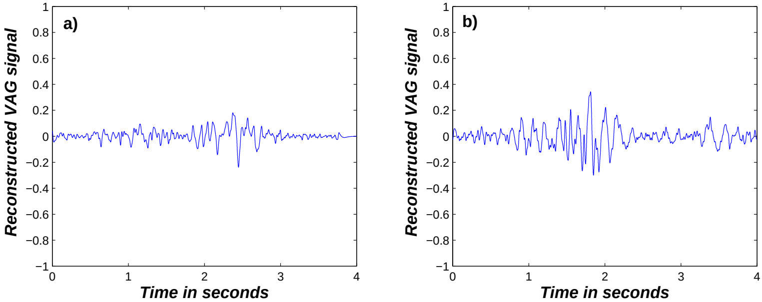

Figure 18: Reconstructed VAG signal of (a) healthy subject and (b) unhealthy subject

Results: Entropy based features

Table 11: Statistical measures of reconstructed VAG signals for entropy based features

	mean ± standard deviation		
Features	healthy	unhealthy	p-value
ApEn	0.00017 ± 0.00019	0.000301 ± 0.00023	0.01262
SampEn	0.00018 ± 0.00020	0.000299 ± 0.00022	0.01421
ShEn	0.23985 ± 0.16550	0.321193 ± 0.16127	0.00969
ReEn	0.05327 ± 0.04180	0.073854 ± 0.04127	0.00297
TsEn	0.05108 ± 0.03896	0.070421 ± 0.03845	0.01505
PeEn	0.88832 ± 0.03444	0.967527 ± 0.02415	0.00042

Results:Analytical representation of VAG signal

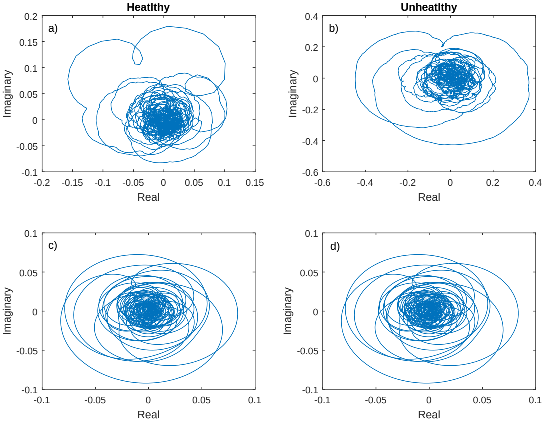

Figure 19: Analytical representation of VAG signal (a) healthy subject (b) unhealthy subject and reconstructed VAG signal of (c) healthy subject and (d) unhealthy subject

Results:CTM

Table 12: Statistical measure for CTM

Healthy	Unhealthy
mean ± std dev	mean ± std dev
0.2369 ± 0.1078	0.2952 ± 0.0894
p-value	
0.0138	

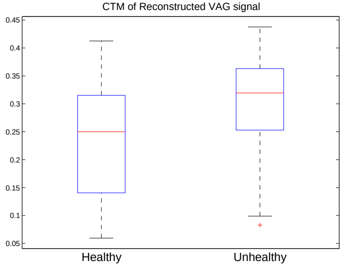

Figure 20: Boxplot for CTM

Results: Classification

Table 13: Classification performance of extracted features from reconstructed VAG signal

Features	ACC	SEN	SPE	PPV	NPV	MCC	FDR	AUC-ROC
ApEn	**0.7640**	0.8947	0.5313	0.7727	0.7391	0.4670	0.2273	0.7647 ± 0.0521
SampEn	**0.8202**	0.9444	0.6286	0.7969	0.8800	0.6228	0.2031	0.7672 ± 0.0506
ShEn	**0.7528**	0.8947	0.5000	0.7612	0.7273	0.4391	0.2388	0.6434 ± 0.0590
ReEn	**0.7191**	0.8793	0.4194	0.7391	0.6500	0.3409	0.2609	0.6583 ± 0.0585
TsEn	**0.7079**	0.8421	0.4688	0.7385	0.6250	0.3361	0.2615	0.6929 ± 0.0624
PeEn	**0.8652**	0.9107	0.7879	0.8793	0.8387	0.7082	0.1207	0.7864 ± 0.0474
Vector	**0.8427**	0.9107	0.7273	0.8500	0.8276	0.6575	0.1500	0.7812 ± 0.0507
CTM	**0.8764**	0.8947	0.8627	0.8293	0.9167	0.7517	0.1707	0.7023 ± 0.0506

Hence, the computational complexity of the proposed system would be

$$O(NlogN) + O(N) + O(N^2) \approx O(N^2) \qquad (1)$$

Results: AUC-ROC

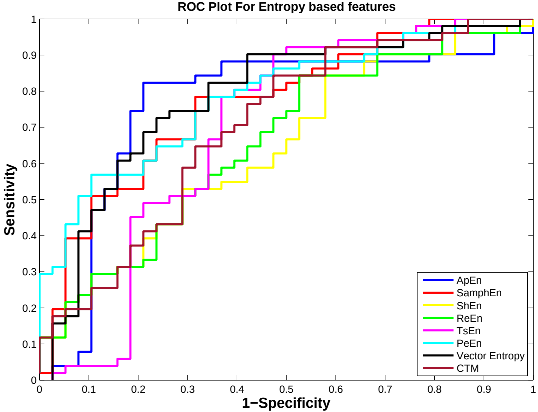

Figure 21: Performance of ROC of extracted features

Results: Comparison of the proposed methodology

Table 14: Comparison of the proposed methodology with the existing non-linear studies

	*EMD[30]	EEMD[15]	**EEMD[44]**	**PeEn**	**CTM**
ACC	85.30%	83.56%	**86.52%**	**86.52%**	**87.64%**
SEN	-	0.9440	**0.9412**	**0.9107**	**0.8947**
SPE	-	0.8000	**0.7632**	**0.7878**	**0.8627**
MCC	-	0.6599	**0.6227**	**0.7082**	**0.7516**
Classifier	-	SVM	**RF**	**LS-SVM**	**LS-SVM**

*Different dataset

Conclusion

- Nonstationary nonlinear signal processing technique "CEEMDAN".
- PeEn gives an accuracy of **86.52%** among the six entropies but the highest classification accuracy has been obtained by CTM: **ACC: 87.64%**.
- The computed time complexity of PeEn/CTM is $O(N)$ and overall computational complexity is $O(N^2)$.

The proposed methodology

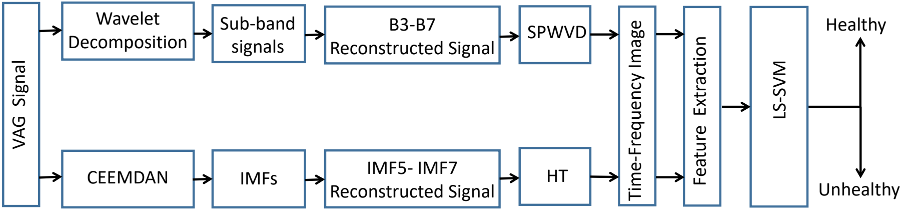

Figure 22: Block diagram for time frequency analysis of knee joint disorders using VAG signals

Saif Nalband, CA.Valliappan, A. Amalin Prince, Anita Agarwal: "Time frequency based feature extraction for the analysis of vibroarthographic signals," (Revised under review) Computers and Electrical Engineering, Elsevier Publication

Results: WPD-SPWVD

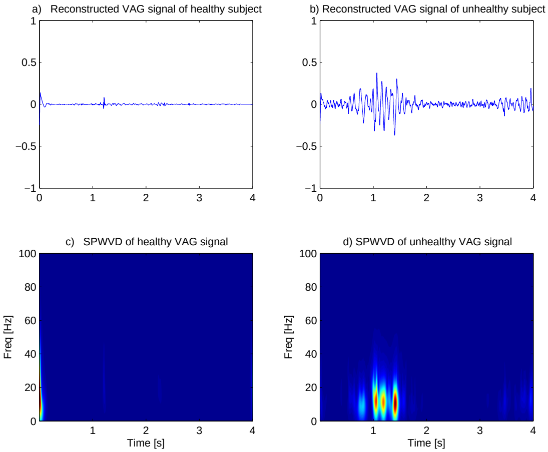

Figure 23: The reconstructed VAG signal obtained from SPWVD (a) healthy subject and (b) unhealthy subject. Time-frequency representation of c) healthy subject and d) unhealthy subject VAG signal

Results: CEEMDAN-HHT

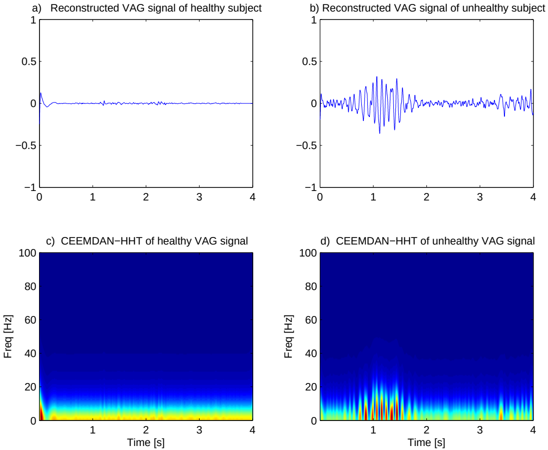

Figure 24: The reconstructed VAG signal obtained from CEEMDAN (a) healthy subject and (b) unhealthy subject. Time-frequency representation of c) healthy subject and d) unhealthy subject VAG signal

Results: Statistical Measures

Table 15: Statistical measures of extracted features using SPWVD and CEEMDAN-HHT

class	Healthy	Unhealthy	
Features	Mean $\pm$ Std	Mean $\pm$ Std	*P-value*
SPWVD			
Mean	0.3461 $\pm$ 0.0662	0.3330 $\pm$ 0.0766	0.3237
Std	1.6886 $\pm$ 0.3238	1.6224 $\pm$ 0.3766	0.3136
skewness	6.7910 $\pm$ 0.0900	6.8137 $\pm$ 0.1127	0.2663
Kurtosis	52.7752 $\pm$ 2.1699	53.4333 $\pm$ 2.6143	0.2050
CEEMDAN-HHT			
Mean	0.3587 $\pm$ 0.0769	0.3373 $\pm$ 0.0670	0.1167
Std	1.7578 $\pm$ 0.3705	1.6550 $\pm$ 0.3224	0.1293
skewness	7.0215 $\pm$ 0.3311	7.1490 $\pm$ 0.3979	0.0629
Kurtosis	58.7469 $\pm$ 8.8681	62.2163 $\pm$ 10.6879	0.0559

Results: Boxplots of extracted features

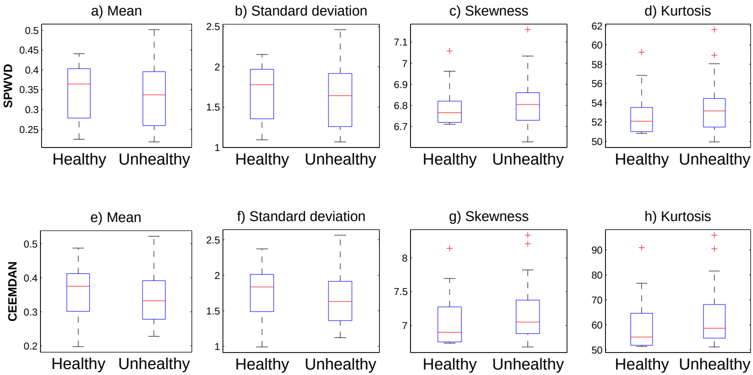

Figure 25: Box plots for features extracted from SPWVD and CEEMDAN-HHT

Results: Classification Performance

Table 16: Classification of features extracted using SPWVD

	Vector	Mean	Std	Skewness	Kurtosis
ACC	**0.7753**	**0.7865**	**0.6667**	**0.7416**	**0.6180**
SEN	0.9091	0.8800	0.8000	0.7586	0.6429
SPE	0.7313	0.7500	0.6389	0.7333	0.6133
PPV	0.5263	0.5789	0.3158	0.5789	0.2368
NPV	0.9608	0.9412	0.9388	0.8627	0.9020
MCC	0.5585	0.5724	0.3343	0.4661	0.1886
FDR	0.4737	0.4211	0.6842	0.4211	0.7632
AUC-ROC	**0.7699 $\pm$ 0.0573**	**0.8945 $\pm$ 0.0622**	**0.7281 $\pm$ 0.0593**	**0.7384 $\pm$ 0.0620**	**0.6744 $\pm$ 0.0594**

Table 17: Classification of features extracted using CEEMDAN-HHT

	Vector	Mean	Std	Skewness	Kurtosis
ACC	**0.8202**	**0.8876**	**0.8764**	**0.7978**	**0.7865**
SEN	0.8750	0.8333	0.9655	0.7500	0.7209
SPE	0.7895	0.9362	0.8333	0.8367	0.8478
PPV	0.7000	0.9211	0.7368	0.7895	0.8158
NPV	0.9184	0.8627	0.9804	0.8039	0.7647
MCC	0.6410	0.7766	0.7569	0.5901	0.5746
FDR	0.3000	0.0789	0.2632	0.2105	0.1842
AUC-ROC	**0.8994 $\pm$ 0.0579**	**0.9383 $\pm$ 0.0615**	**0.9494 $\pm$ 0.0617**	**0.8127 $\pm$ 0.0617**	**0.8519 $\pm$ 0.0568**

Results: AUC-ROC

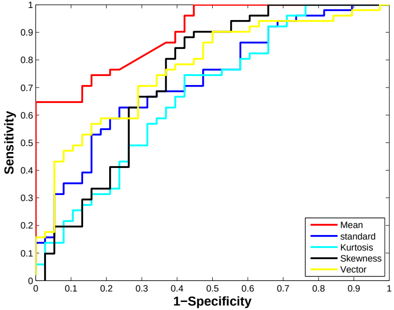

(a) SPWVD

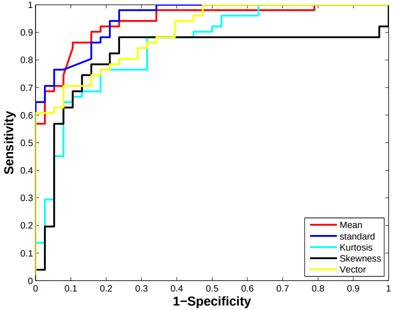

(b) CEEMDAN-HHT

Figure 26: ROC plot for statistical features obtained from time frequency distribution

Comparison of the proposed methodology

Table 18: Comparison of the proposed methodology with existing TFD

Methodology	MP [25]	MP [26]	MLD [27]	*EMD-HHT [30]	**CEEMDAN**
ACC	77.8	68.9	79.8	85.3	**88.76**
SEN	-	-	-	-	**0.833**
SPE	-	-	-	-	**0.9362**
MCC	-	-	-	-	**0.7766**
Classifier	DA	LR	LDA	-	**LS-SVM**
No of samples	37	90	89	35	**89**

*Different dataset

Conclusion

- Time-frequency based techniques namely SPWVD and CEEMDAN-HHT were studied.
- The time-frequency representation has been considered as time-frequency image
- CEEMDAN-HHT performed better with respect to SPWVD by giving the highest accuracy of **88.76%**.

Outcome of Thesis

The methodologies carried out in this research has been based on nonstationary signal processing techniques and were followed by feature extraction techniques.

Table 19: Summary of Thesis Methodologies

	Methodology 1	Methodology 2	Methodology 3	Methodology 4
Preprocessing	WPD	WPD	CEEMDAN	WPD-SPWVD & CEEMDAN-HHT
Feature extraction	Entropies + RQA	Entropies + RQA	Entropies	Statistical Features
Feature Selection	-	GA & ApA	-	-
Classifier	LS-SVM			

Summary of the thesis work

Table 20: Summary of the thesis work:Results

Features	No of features	ACC	SEN	MCC	AUC-ROC	Chapter
Entr + RQA (SB + Recon)	60	69.66%	0.5888	0.4337	0.7822 ± 0.0471	
Entr + RQA (SB)	50	80.90%	0.9216	0.8621	0.8606 ± 0.0397	3
Entr + RQA (Recon)	10	84.27%	0.9020	0.8529	0.8560 ± 0.0427	
FS by GA	8	82.02%	0.7254	0.6707	0.8754 ± 0.0347	4
FS by ApA	5	**85.39%**	0.9272	0.6868	$\mathbf{0.9252} \pm \mathbf{0.0261}$	
Entropies (vector)	6	84.27%	0.9107	0.6575	0.7812 ± 0.0507	
PeEn	1	**86.52%**	0.9107	0.7082	0.7864 ± 0.0474	5
CTM	1	**87.64%**	0.8947	0.7517	0.7023 ± 0.0506	
SPWVD	4	77.53%	0.9091	0.5585	0.7699 ± 0.0573	
CEEMDAN-HHT	4	82.02%	0.8750	0.6410	0.8994 ± 0.0579	6
Mean(CEEMDAN-HHT)	1	**88.76%**	0.8333	0.7766	$\mathbf{0.9383} \pm \mathbf{0.0615}$	

Future Scope

1. Larger number of samples in dataset, a cloud based approach.
2. Deep learning based convolution neural network (CNN).
3. Data acquisition could be carried out by placing multiple sensors.
4. Developing a prototype knee joint diagnostics system

List of Publications

Journal Publication

1) S. Nalband, A. Sundar, A.A. Prince, & A. Agarwal. "Feature selection and classification methodology for the detection of knee-joint disorders," Computer methods and programs in biomedicine, 127, 94-104, 2016. *Elsevier Publication* **SCI: Impact Factor: 2.503**
2) S. Nalband, A.A. Prince, & A. Agarwal. "An entropy based feature extraction and classification of Vibroarthographic signal using improved complete ensemble empirical mode decomposition with adaptive noise," (Manuscript Accepted: In Press) *IET Science, Measurement & Technology* **SCI: Impact Factor: 1.26**
3) S. Nalband, Valliappan C.A, A.A. Prince, & A. Agarwal. "Time frequency based feature extraction for the analysis of vibroarthographic signals", (Revised under review) *Computers and Electrical Engineering, Elsevier Publication*

Conference Publications

1) S.Nalband, CA.Valliappan, R.Gupta, A.A.Prince, and A.Agarwal, "Feature Extraction and Classification of Knee Joint Disorders Using Hilbert Huang Transform," 14th Annual IEEE Conference of ECTI Society, (ECTI-CON 2017) IEEE, pp. 266-269, June 27-30, 2017 Phuket, Thailand.**(Scopus)**
2) S. Nalband, R.R.Sreekrishna R.R. and A.A.Prince "Analysis of Knee Joint Vibration Signals Using Ensemble Empirical Mode Decomposition," Elsevier Procedia Computer Science, vol.89, pp. 820-827, 2016. **(Scopus)**
3) R.R.Sreekrishna, S. Nalband and A.A.Prince. "Real Time Cascaded Moving Average Filter for Detrending of Electroencephalogram Signals," 5th IEEE International Conference on Communication and Signal Processing (ICCSP'16), p.p. 0745 - 0750, April 2016, Chennai, India, IEEE. **(Scopus)**

Bibliography I

[1] V. Vigorita, B. Ghelman, and D. Mintz, *Orthopaedic Pathology*.
M - Medicine Series, Lippincott Williams & Wilkins, 2008.

[2] C. Prakash, A. Khanvilkar, A. Deshpande, A. Agashe, A. Mankar, and Pathak.Dhananjay, "To find out the prevalence of knee osteoarthritis in the indian population and the factors associated with it: Indian orthopaedic association," November 2013.

[3] G. McCoy, J. McCrea, D. Beverland, W. Kernohan, and R. Mollan, "Vibration arthrography as a diagnostic aid in diseases of the knee. a preliminary report," *Journal of Bone and Joint Surgery, British Volume*, vol. 69-B, no. 2, pp. 288–293, 1987.

[4] Y. F. Wu, *Knee Joint Vibroarthrographic Signal Processing and Analysis*.
Springer-Verlag, 2015.

[5] M. Chu, I. Gradisar, and R. Mostardi, "A noninvasive electroacoustical evaluation technique of cartilage damage in pathological knee joints," *Medical and Biological Engineering and Computing*, vol. 16, pp. 437–442, Jul 1978.

[6] G. Kernohan and R. Mollan, "Microcomputer analysis of joint vibration," *Journal of Microcomputer Applications*, vol. 5, no. 4, pp. 287–296, 1982.

[7] A. R. Webb, *Statistical pattern recognition*.
John Wiley & Sons, second edition ed., 2003.

[8] Y. T. Zhang, R. Rangayyan, G. Bell, and C. Frank, "Adaptive cancellation of muscle contraction interference in vibroarthrographic signals," *IEEE Transactions on Biomedical Engineering*, vol. 41, no. 2, pp. 181–191, 1994.

[9] S. Krishnan, R. M. R. Rangayyan, G. G. D. Bell, C. B. Frank, and K. O. Ladly, "Adaptive filtering, modelling and classification of knee joint vibroarthrographic signals for non-invasive diagnosis of articular cartilage pathology," *Medical and Biological Engineering and Computing*, vol. 35, no. 6, pp. 677–684, 1997.

[10] Y. Wu, S. Cai, M. Lu, S. Yang, F. Zheng, N. Xiang, J. He, and Z. Zhong, "Noise Cancellation in Knee Joint Vibration Signals Using a Time-Delay Neural Filter and Signal Power Error Minimization Method," vol. 8, pp. 912–919, 2013.

Bibliography II

[11] J.-C. Chen, P.-C. Tung, S.-F. F. Huang, S.-L. L. Lin, S.-W. Wu, and S.-L. L. Lin, “Extraction and screening of knee joint vibroarthrographic signals using the independent component analysis method,” *International Journal of Innovative Computing, Information and Control*, vol. 8, no. 11, pp. 7501–7518, 2012.

[12] A. Sundar, C. Das, and V. Pahwa, *Denoising Knee Joint Vibration Signals Using Variational Mode Decomposition*, pp. 719–729.
New Delhi: Springer India, 2016.

[13] Y. Wu, S. Cai, F. Xu, L. Shi, and S. Krishnan, *Chondromalacia Patellae Detection by Analysis of Intrinsic Mode Functions in Knee Joint Vibration Signals*, pp. 493–496.
Berlin, Heidelberg: Springer Berlin Heidelberg, 2013.

[14] Y. F. Wu, S. Yang, F. Zheng, S. Cai, M. Lu, and M. Wu, “Removal of artifacts in knee joint vibroarthrographic signals using ensemble empirical mode decomposition and detrended fluctuation analysis.,” *Physiological measurement*, vol. 35, no. 3, pp. 429–39, 2014.

[15] Y. Wu, P. Chen, X. Luo, H. Huang, L. Liao, Y. Yao, M. Wu, and R. M. Rangayyan, “Quantification of knee vibroarthrographic signal irregularity associated with patellofemoral joint cartilage pathology based on entropy and envelope amplitude measures,” *Computer Methods and Programs in Biomedicine*, vol. 130, pp. 1–12, 2016.

[16] S. Tavathia, R. M. Rangayyan, C. B. Frank, G. D. Bell, and K. O. Ladly, “Analysis of knee vibration signals using linear prediction,” *IEEE transactions on biomedical engineering*, vol. 39, no. 9, pp. 959–70, 1992.

[17] Z. M. K. Moussavi, R. M. Rangayyan, G. D. Bell, C. B. Frank, K. O. Ladly, and Y. T. Zhang, “Screening of vibroarthrographic signals via adaptive segmentation and linear prediation modeling,” *IEEE Transactions on Biomedical Engineering*, vol. 43, no. 1, pp. 15–23, 1996.

[18] S. Krishnan, R. M. Rangayyan, G. D. Bell, C. B. Frank, and K. O. Ladly, “Screening of knee joint vibroarthrographic signals by statistical pattern analysis of dominant poles,” *Proceedings of 18th Annual International Conference of the IEEE Engineering in Medicine and Biology Society*, vol. 3, no. 2, pp. 968–969, 1996.

Bibliography III

[19] R. M. Rangayyan and Y. F. Wu, “Screening of knee-joint vibroarthrographic signals using statistical parameters and radial basis functions,” *Medical and Biological Engineering and Computing*, vol. 46, no. 3, pp. 223–232, 2008.

[20] R. M. Rangayyan and Y. Wu, “Screening of knee-joint vibroarthrographic signals using probability density functions estimated with Parzen windows,” *Biomedical Signal Processing and Control*, vol. 5, no. 1, pp. 53–58, 2010.

[21] Y. Wu, S. Cai, S. Yang, F. Zheng, and N. Xiang, “Classification of Knee Joint Vibration Signals Using Bivariate Feature Distribution Estimation and Maximal Posterior Probability Decision Criterion,” *Entropy*, vol. 15, no. 4, pp. 1375–1387, 2013.

[22] S. Cai, S. Yang, F. Zheng, M. Lu, Y. Wu, and S. Krishnan, “Knee joint vibration signal analysis with matching pursuit decomposition and dynamic weighted classifier fusion,” *Computational and Mathematical Methods in Medicine*, vol. 2013, 2013.

[23] R. M. Rangayyan, F. Oloumi, Y. Wu, and S. Cai, “Fractal analysis of knee-joint vibroarthrographic signals via power spectral analysis,” *Biomedical Signal Processing and Control*, vol. 8, no. 1, pp. 23–29, 2013.

[24] S. Yang, S. Cai, F. Zheng, Y. Wu, K. Liu, M. Wu, Q. Zou, and J. Chen, “Representation of fluctuation features in pathological knee joint vibroarthrographic signals using kernel density modeling method,” *Medical Engineering and Physics*, vol. 36, no. 10, pp. 1305–1311, 2014.

[25] S. Krishnan, R. M. Rangayyan, G. G. D. Bell, and C. B. Frank, “Time-frequency signal feature extraction and screening of knee joint vibroarthrographic signals using the matching pursuit method,” in *Engineering in Medicine and Biology Society, 1997. Proceedings of the 19th Annual International Conference of the IEEE*, vol. 3, pp. 1309–1312, IEEE, 1997.

[26] S. Krishnan, R. M. Rangayyan, G. D. Bell, and C. B. Frank, “Adaptive time-frequency analysis of knee joint vibroarthrographic signals for noninvasive screening of articular cartilage pathology,” *IEEE Transactions on Biomedical Engineering*, vol. 47, no. 6, pp. 773–783, 2000.

[27] K. Umapathy and S. Krishnan, “Modified local discriminant bases algorithm and its application in analysis of human knee joint vibration signals,” *IEEE Transactions on Biomedical Engineering*, vol. 53, no. 3, pp. 517–523, 2006.

Bibliography IV

[28] Y. Wu and S. Krishnan, "Classification of knee-joint vibroarthrographic signals using time-domain and time-frequency domain features and least-squares support vector machine," in *Digital Signal Processing, 2009 16th International Conference on*, pp. 1–6, IEEE, 2009.

[29] K. S. Kim, J. H. Seo, J. U. Kang, and C. G. Song, "An enhanced algorithm for knee joint sound classification using feature extraction based on time-frequency analysis," *Computer methods and programs in biomedicine*, vol. 94, no. 2, pp. 198–206, 2009.

[30] J.-C. Chen, P.-C. Tung, S.-F. Huang, S.-W. Wu, S.-L. Lin, and K.-L. Tu, "Extraction and screening of knee joint vibroarthrographic signals using the empirical mode decomposition method," *International Journal of Innovative Computing, Information and Control*, vol. 9, no. 6, pp. 2689–2700, 2013.

[31] D. Baczkowicz, E. Majorczyk, and K. Krecisz, "Age-related impairment of quality of joint motion in vibroarthrographic signal analysis," *BioMed Research International*, vol. 2015, 2015.

[32] R. M. Rangayyan and Y. Wu, "Analysis of vibroarthrographic signals with features related to signal variability and radial-basis functions," *Annals of Biomedical Engineering*, vol. 37, no. 1, pp. 156–163, 2009.

[33] T. Mu, A. K. Nandi, and R. M. Rangayyan, "Strict 2-surface proximal classification of knee-joint vibroarthrographic signals," in *Annual International Conference of the IEEE Engineering in Medicine and Biology - Proceedings*, pp. 4911–4914, 2007.

[34] Y. Wu and S. Krishnan, "Combining least-squares support vector machines for classification of biomedical signals: a case study with knee-joint vibroarthrographic signals," *Journal of Experimental & Theoretical Artificial Intelligence*, vol. 23, no. 1, pp. 63–77, 2011.

[35] K. Liu, X. Luo, S. Yang, S. Cai, F. Zheng, and Y. Wu, "Classification of knee joint vibroarthrographic signals using k-nearest neighbor algorithm," in *Canadian Conference on Electrical and Computer Engineering*, IEEE, 2014.

[36] D. Ingrid, *Ten lectures on wavelets: CBMS-NSF Regional Conference Series in Applied Mathematics*. SIAM, Philadelphia, USA, 1992.

Bibliography V

[37] M. A. Colominas, G. Schlotthauer, and M. E. Torres, "Improved complete ensemble EMD: A suitable tool for biomedical signal processing," *Biomedical Signal Processing and Control*, vol. 14, no. 1, pp. 19–29, 2014.

[38] C. L. Webber and J. P. Zbilut, "Dynamical assessment of physiological systems and states using recurrence plot strategies," *Journal of Applied Physiology*, vol. 76, no. 2, pp. 965–973, 1994.

[39] M. E. Cohen, D. L. Hudson, and P. Ć. Deedwania, "Applying continuous chaotic modeling to cardiac signal analysis," *IEEE Engineering in Medicine and Biology Magazine*, vol. 15, no. 5, pp. 97–102, 1996.

[40] D. E. Goldberg, *Genetic Algorithms in Search, Optimization, and Machine Learning*, vol. Addison-We. 1989.

[41] R. Agrawal, H. Mannila, R. Srikant, H. Toivonen, A. I. Verkamo, *et al.*, "Fast discovery of association rules," *Advances in knowledge discovery and data mining*, vol. 12, pp. 307–328, 1996.

[42] F. Hlawatsch, T. G. Manickam, R. L. Urbanke, and W. Jones, "Smoothed pseudo-Wigner distribution, Choi-Williams distribution, and cone-kernel representation: Ambiguity-domain analysis and experimental comparison," *Signal Processing*, vol. 43, no. 2, pp. 149–168, 1995.

[43] N. E. Huang, Z. Shen, S. R. Long, M. C. Wu, H. H. Shih, Q. Zheng, N.-C. Yen, C. C. Tung, and H. H. Liu, "The empirical mode decomposition and the hilbert spectrum for nonlinear and non-stationary time series analysis," in *Proceedings of the Royal Society of London A: Mathematical, Physical and Engineering Sciences*, vol. 454, pp. 903–995, The Royal Society, 1998.

[44] S. Nalband, R. Sreekrishna, and A. A. Prince, "Analysis of Knee Joint Vibration Signals Using Ensemble Empirical Mode Decomposition," *Procedia Computer Science*, vol. 89, pp. 820–827, 2016.

Acknowledgements

- Supervisor: Dr. A.Amalin Prince
- Co-Supervisor: Dr. Anita Agrawal
- DAC Members:
  - Senior Prof. Raghurama Gunaje - Director, BITS-Pilani, K. K. Birla Goa Campus
  - Prof. K R Anupama
- Dr. Gautam Bacher Convener, Departmental Research Committee
- Dr. Nitin Sharma, Prof. M. K. Deshmukh
- Academic Research Division, all the faculties of department, technical staff and fellow research scholars
- Vijay Patil and "Reconfigurable and computing Lab"
- Prof. R.M.Rangayyan
- My lab colleagues Mr. Jay Kumar and Mr. Gibin George for their support.
- Mr. Adtiya Sundar, Mr. Valliappan C.A and other students who have worked in the lab
- Lab mates for their cooperation, Friends and Family.

Thank You